Proceedings of the E-MRS Fall Meeting, Symposium H: Warsaw, Poland, September 19–23, 2011

A Photoacoustic Study of Xenon Implantation in $CuInSe_2$

F.Z. Satour[a], A. Zegadi[a] and A. Merabet[b,*]

[a]LCCNS, Département d'Electronique, Faculté de Technologie, Université Ferhat Abbas — Sétif Sétif 19000, Algeria

[b]LPMMM, I.O.M.P., Université Ferhat Abbas — Sétif, Sétif 19000, Algeria

In this paper, we report a study on the optical properties of xenon ion implanted $CuInSe_2$ single crystals using a high resolution near-infrared photoacoustic spectrometer of the gas-microphone type. Samples of high quality of $CuInSe_2$, p-type conducting, have been implanted with Xe^+ at 40 keV with doses of 5×10^{15}, 10^{16} and 5×10^{16} ions/cm^2. Photoacoustic spectra have been measured before and after implantation. A newly developed theoretical model based on a two-layer sample configuration has been used to single out the spectral dependence of the absorption coefficient of the implanted layer from that of the substrate. The absorption spectra were used to evaluate the gap energy and to establish ionization energies for several shallow and deep defect states. The resulting effects following the introduction of xenon into $CuInSe_2$ at different doses are discussed in the light of published literature.

PACS: 81.70.Cv, 78.20.Ci, 78.40.Fy, 61.82.Fk, 71.55.−i

1. Introduction

Among the leading candidates being investigated nowadays in solar energy research are the chalcopyrite compound $CuInSe_2$ (CIS) and its alloys $Cu(In,Ga)Se_2$ (CIGS). Recent progress in laboratory research of solar cells based on these materials as the absorber layer has achieved efficiencies in excess of 20% [1]. $CuInSe_2$ is reported to be resistant to radiation damage and as such could provide photovoltaic technology for long-term projects in space. Yet, little is known on the mechanisms responsible for the material hardness. Of all the species investigated so far, xenon ions are of particular significance. This inert gas is not to be electrically active and should allow an investigation of the induced damage to be made without the complication of extrinsic doping.

Recently, photoacoustic spectroscopy (PAS) has emerged as a potential and reliable technique in the analysis of the optical properties of semiconductors [2]. In addition, it is contactless and nondestructive; PAS is unique in offering the possibility for depth profiling analysis.

In this paper, we present the results of a study on the optical properties of xenon implanted p-conducting $CuInSe_2$ single crystals with doses of 5×10^{15}, 10^{16} and 5×10^{16} ions/cm^2 at the energy of 40 keV. Of interest to us are the changes induced on the intrinsic defect structure observed in the subgap region of CIS following xenon implantation.

2. Experiment

The photoacoustic spectrometer has been described in detail elsewhere [3]. Basically, a sample irradiated by a periodically modulated light beam gets heated by the nonradiative processes following light absorption. This heating gives rise to both temperature and pressure fluctuations that can be detected by thermal, acoustic, or both, sensing devices [4]. The photoacoustic cell, which is rectangular in shape, is made of stainless steel. Its schematic diagram is shown in Fig. 1, in which a double-layer sample is assumed.

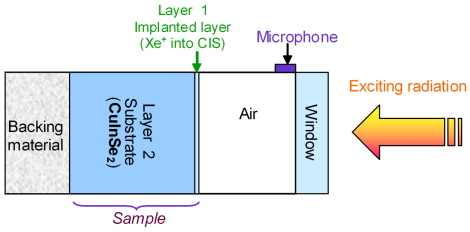

Fig. 1. Schematic diagram of the photoacoustic cell.

p-type conducting $CuInSe_2$ single crystal samples, the thicknesses of which are in the order of 500 μm, of high quality grown by using the vertical Bridgman technique have been used. These have been prepared using standard techniques (polishing and etching) [5]. The composition of the samples was in the range of 22.5 to 23.5 at.% copper, 26.5 to 27.5 at.% indium and 49.5 to 50.5 at.% selenium as determined by electron microprobe measurements. Such compositions can lead to p-type and n-type conducting in dependence on the specific intrinsic defect equilibrium [6].

The ion separator of Freeman source type at Salford University (UK) was used to implant the sample at a current density of 2–5 μA cm^{-2}. The irradiations were carried out at room temperature with the sample set normal to the beam.

Finally, the PA spectra measured before and after implantation are corrected for the spectral distribution of the optical system, the microphone, and the cell by nor-

* corresponding author; e-mail: merabet_abdelali@yahoo.fr

malizing the response of the specimens to that of fine particles of carbon black. All spectra were obtained at room temperature at a modulating frequency of 112 Hz.

3. Results and discussion

An ion range profile for 40 keV Xe^+ implants into CIS is shown in Fig. 2. This profile is generated using SRIM--2010 software [7], in which a CIS structure with a density of 5.77 g/cm^3 is assumed. The simulation was carried out for 10000 ions over a layer thickness of 600 Å. The concentration tail of the implants extends to a depth of 400 Å. This agrees well with the experimental observations of Mullan and co-workers [8].

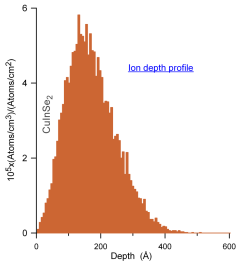

Fig. 2. Depth profile simulation from SRIM-2010.

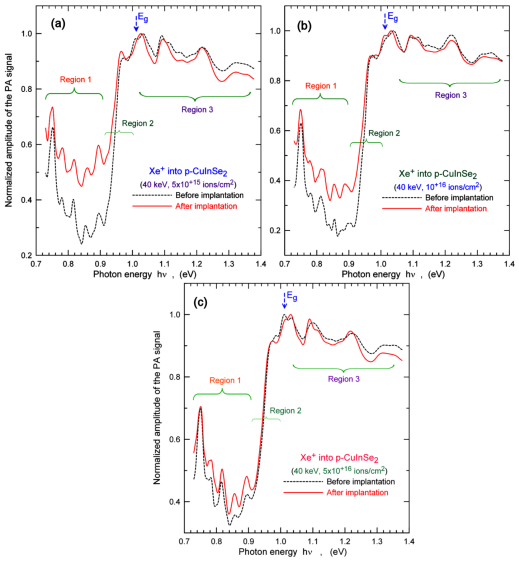

Fig. 3. The normalized photoacoustic amplitude as a function of the photon energy measured before and after Xe^+ implantation into $CuInSe_2$ samples at 40 keV with the doses (a) 5×10^{15} ions/cm^2, (b) 10^{16} ions/cm^2, (c) 5×10^{16} ions/cm^2.

Figure 3a–c shows the effect of xenon ion implantation in $CuInSe_2$ by comparing PA spectra measured before and after implantation for three doses, respectively. The response measured of the sample after the implantation arises from both layers (i.e. the implanted layer and a part of the substrate). Changes are observed all over the spectral range.

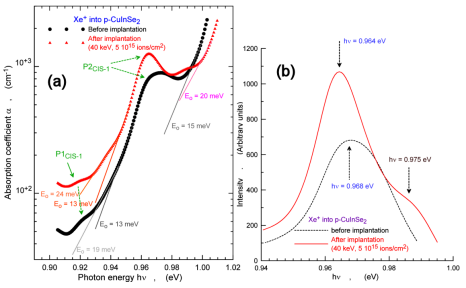

Fig. 4. (a) The spectral dependence of the absorption coefficient near to the fundamental edge calculated from the data of Fig. 3(a) of the sample before and after implantation (dose: 5×10^{15} ions/cm^2). (b) The relative intensity spectral dependence of the shoulder $P2_{\mathrm{CIS}-1}$.

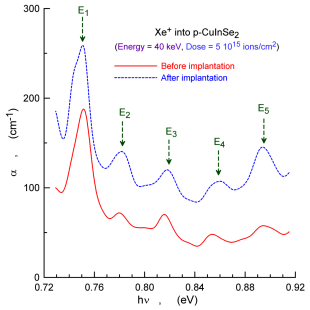

Fig. 5. Comparative plots of the absorption coefficients showing deeper state transitions.

Three distinct regions are observed in all spectra:

- Region 1 ($0.7 \le h\nu \le 0.92$ eV): the region of transparency in which several peaks are observed. These have been associated with transitions between defect states and the conduction/valence bands [5].
- Region 2 ($0.92 \le h\nu \le 1.02$ eV): the fundamental edge region which shows clearly the direct band to band transition of $CuInSe_2$. The maximum coincides well with the reported value of the gap energy for $CuInSe_2$ single crystals [9], $E_g = 1.01$ eV, indicated by an arrow in the figures. The xenon implantation process is seen to affect the shoulder which is close to the maximum of the edge. Only the sample (CIS-1) implanted with the dose 5×10^{15} ions/cm^2 had a conversion type into n following the implantation process.
- Region 3 ($1.02 \le h\nu \le 1.4$ eV): the saturation region in which the whole incident light beam is absorbed within a thin layer of thickness in the order of the optical diffusion length [5]. Minor changes are observed between the spectra.

Recently, we derived a theoretical relation based on a two-layer sample in application to implanted semiconductors which allows extracting the response that arises

from the implanted layer alone knowing its thickness and the response before implantation.

Figure 4 shows the resulting resolved absorption coefficient spectrum of the implanted layer with the dose of 5×10^{15} ions/cm^2 together with the sample spectrum prior to its implantation in the region close to the absorption fundamental edge. The introduction of xenon is seen to affect the shoulder, $P2_{\mathrm{CIS}-1}$. The central photon energy position of this feature is extracted and the result is displayed in Fig. 4b. Above and below this shoulder the absorption spectrum exhibits exponential dependences indicating the presence of several shallow energy levels some of which are due to xenon.

Figure 5 shows plots of the absorption coefficient derived from the sections of the PA spectrum below the energy gap of the sample before and after the implantation process (dose: 5×10^{15} ions/cm^2) to provide a basis for comparison. Five major peaks are resolved in the absorption spectra with varying intensities. These are associated with transitions between nonradiative defect states and the conduction/valence bands.

A summary on the defect activation and ionization energies derived from the determined value for the gap energy thus detected and possible activities according to the literature [10] of the sample prior to implantation are listed in Table.

TABLE

Defect levels together with their ionization energies by using the determined gap energy E_{g} of the sample prior to implantation.

	Defect levels		Electrical activity and attribution [10]
	Peak $h\nu$ position [eV]	Ionization energy [meV]	
$E_{\mathrm{g}} = 1.001 \pm 0.002$ eV			
L_1		8 ± 5	D $\rightarrow$ V_{Se}
A_2	0.981	20 ± 3	A $\rightarrow$ V_{Cu} $(-/0)$
A_1	0.970	30 ± 1	A $\rightarrow$ V_{Cu} $(-/0)$
E_1	0.750	251	A $\rightarrow$ Cu_{In} $(-/0)$
E_2	0.782	219	D $\rightarrow$ Cu_i $(0/+)$ or In_{Cu} $(0/+)$
E_3	0.816	185	A $\rightarrow$ V_{In} $(-/0)$
E_4	0.858	143	D $\rightarrow$ Cu_i $(0/+)$ or In_{Cu} $(0/+)$
E_5	0.896	105	A $\rightarrow$ Cu_{In} + Cu_i $(-/0)$

* A — acceptor, D — donor

It is to be noted that the introduction of xenon into $CuInSe_2$ has created three main changes. The first one is the shallow level A_2 attributed in the literature to the acceptor V_{Cu} and appearing close to the fundamental edge, has replaced the shallow level L_1 and attributed to the defect V_{Se}. In fact, and this is the second change noted, this defect state could be the same level as the defect state A_2 which has disappeared from the spectrum following the implantation process. The third change is the new level state detected at low dose having the ionization energy of 223 meV. It coincides well with the one reported by Tomlinson and co-workers [9] and attributed to the acceptor state Cu_{In}.

4. Conclusion

We have presented a study on the optical properties of xenon implanted $CuInSe_2$ single crystals. We have extracted the spectrum of the implanted layer alone from that of the substrate. This has allowed us to follow the evolution of defects populations and to analyze the effects produced on the optical properties of $CuInSe_2$ following its implantation with xenon ions. The results have been compared to data published and good agreement has been found.

References

[1] I. Repins, M.A. Contreras, B. Egaas, C. DeHart, J. Scharf, C.L. Perkins, B. To, R. Noufi, *Prog. Photovolt.* **16**, 235 (2008).

[2] H. Benamrani, F.Z. Satour, A. Zegadi, A. Zouaoui, *J. Lumin.* **132**, 305 (2011).

[3] A. Zegadi, M.A. Slifkin, R.D. Tomlinson, *Rev. Sci. Instrum.* **65**, 2238 (1994).

[4] A. Rosencwaig, *Photoacoustics and Photoacoustic Spectroscopy*, Wiley, New York 1980.

[5] A. Zegadi, M.A. Slifkin, M. Djamin, R.D. Tomlinson, H. Neumann, *Solid State Commun.* **83**, 587 (1992).

[6] H. Neumann, R.D. Tomlinson, *Sol. Cells* **28**, 301 (1990).

[7] J.F. Ziegler, *SRIM-2010*, `srim.org` .

[8] C.A. Mullan, C.J. Kiely, M.V. Yakushev, M. Imaneith, R.D. Tomlinson, A. Rockett, *Inst. Phys. Conf. Ser.* **134**, 547 (1993).

[9] R.D. Tomlinson, M.V. Yakushev, H. Neumann, *Cryst. Res. Technol.* **28**, 267 (1993).

[10] S.B. Zhang, Su-Huai Wei, A. Zunger, H. Katayama-Yoshida, *Phys. Rev. B* **57**, 9642 (1998).